PAPER • OPEN ACCESS

A minimal spatial cell lineage model of epithelium: tissue stratification and multi-stability

To cite this article: Wei-Ting Yeh and Hsuan-Yi Chen 2018 *New J. Phys.* **20** 053051

New Journal of Physics
The open access journal at the forefront of physics

Deutsche Physikalische Gesellschaft DPG
IOP Institute of Physics

Published in partnership with: Deutsche Physikalische Gesellschaft and the Institute of Physics

OPEN ACCESS

RECEIVED
18 January 2018

REVISED
1 May 2018

ACCEPTED FOR PUBLICATION
4 May 2018

PUBLISHED
23 May 2018

PAPER

A minimal spatial cell lineage model of epithelium: tissue stratification and multi-stability

Wei-Ting Yeh[1,2,3] **and Hsuan-Yi Chen**[2,4]

[1] Department of Physics, Nagoya University, Nagoya, 464-8602, Japan
[2] Department of Physics, National Central University, Jhongli, 32001, Taiwan
[3] Institute of Atomic and Molecular Sciences, Academia Sinica, Taipei, 10617, Taiwan
[4] Institute of Physics, Academia Sinica, Taipei, 11529, Taiwan

E-mail: wtyeh1989@gmail.com **and** hschen@phy.ncu.edu.tw

Keywords: biological tissues, active matter, hydrodynamic theory

Abstract

A minimal model which includes spatial and cell lineage dynamics for stratified epithelia is presented. The dependence of tissue steady state on cell differentiation models, cell proliferation rate, cell differentiation rate, and other parameters are studied numerically and analytically. Our minimal model shows some important features. First, we find that morphogen or mechanical stress mediated interaction is necessary to maintain a healthy stratified epithelium. Furthermore, comparing with tissues in which cell differentiation can take place only during cell division, tissues in which cell division and cell differentiation are decoupled can achieve relatively higher degree of stratification. Finally, our model also shows that in the presence of short-range interactions, it is possible for a tissue to have multiple steady states. The relation between our results and tissue morphogenesis or lesion is discussed.

1. Introduction

A very special class of active soft matter is biological tissues [1]. *In vitro*, active cell events drive the evolution of a tissue and it is often a good system to illustrate general ideas in active matter hydrodynamic theories [2, 3]. On the other hand, mature biological tissues *in vivo* are robust, with well-defined spatial structure and biological functions that are not easily changed by external perturbations [4]. Such robustness is an important feature for systems with biological functions.

Several kinds of cell–cell interactions exist to make biological tissues robust against perturbations. In principle, these interactions can be short-range interactions due to cell–cell direct contact [5], or interactions with range large compared to the size of a cell. Examples of such relatively long-range interactions include morphogen/nutrient-mediated [6] and stress-sensing [7] interactions. Quantitatively distinguish how different interactions affect tissue dynamics is an important issue in biophysics.

In this *article* we focus on stratified epithelia, epithelia with multiple layers of cells often found in skin and many mucous membranes. A well-studied example is the olfactory epithelium of mouse [6]. Under a microscope, an olfactory epithelium shows proliferative cells above the basal membrane and differentiated cells below the apical surface [8]. This is shown in the cartoon picture in figure 1. Intuitively this structure protects the proliferative cells from leaving the epithelium due to external influences, and places differentiated cells close to the apical surface to perform their biological functions. To maintain proper portion of proliferative and differentiated cells, the proliferative cells and differentiated cells form a lineage shown in figure 2(a), it shows that cell differentiation and self-renew of proliferative cells need to be regulated at proper rates to compensate the lose of differentiated cells due to apoptosis [9].

In the olfactory epithelium, it has been proposed that cell differentiation only happens during cell division. When a proliferative cell divides, each daughter cell has a chance p_S to be a proliferative cell, and a chance $1 - p_S$ to be a differentiated cell [6]. By regulating p_S and cell proliferation rate, it is possible for an olfactory epithelium to maintain a stable homeostasis state [10]. This model, in which cell differentiation is coupled to cell

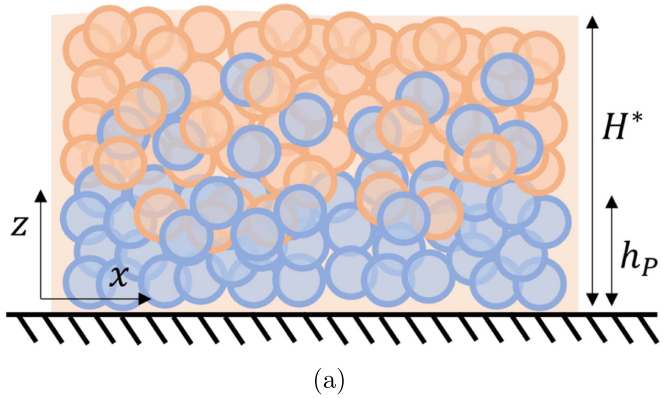

Figure 1. A cartoon picture of a stratified epithelium. The basal membrane is located at the *xy* plane. The apical surface is located at $z = H^*$ when the tissue is in the steady state. The proliferative cells (blue circles) are located close to the basal membrane and the differentiated cells (orange circles) are close to the apical surface. In the steady state the local proportion of the proliferative cells is a decreasing function of z. In particular, for a normal stratified epithelium, one can identify a proliferative cell niche near the basal membrane with a characteristic thickness h_P.

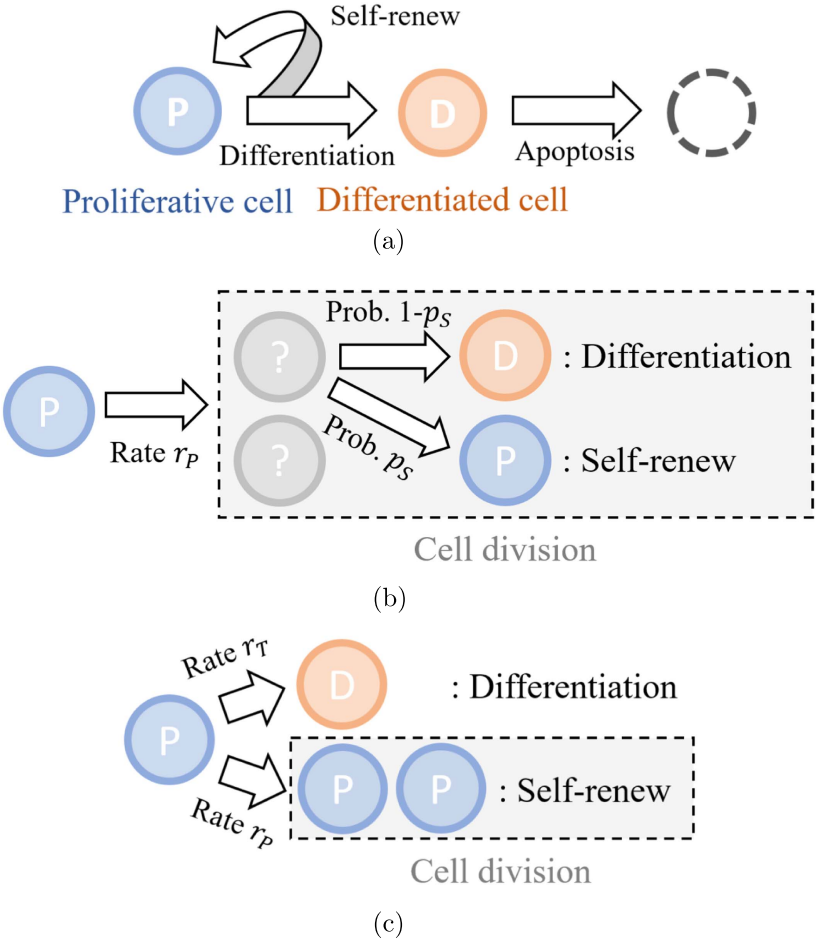

Figure 2. (a) Illustration of the concept of cell lineage. A proliferative cell can undergo cell division and cell differentiation. Self-renew of the proliferative cells is achieved when the daughter cells are also proliferative cells. A differentiated cell will eventually die due to cell apoptosis. The detailed mechanism of cell division and differentiation may be different for different tissues. (b) This model assumes that cell differentiation can take place only during cell division. A daughter cell has a probability p_S to become a proliferative cell, and there is a probability $1 - p_S$ for the daughter cell to be a differentiated cell. As a result, cell differentiation is coupled to cell division. (c) This model assumes that cell division and differentiation are decoupled. At any instance, the proliferative cells have a certain chance to differentiate (with rate r_T) or undergo cell division which produces two proliferative cells (with rate r_P).

proliferation, is shown schematically in figure 2(b). On the other hand, experiments and theories [11–13] on the monolayer epithelium which covers the intestine crypts show that the only mechanism that can explain the stem-cell clone size distribution is different. This model, as illustrated in figure 2(c), assumes that cell differentiation is decoupled from cell proliferation. That is, when a proliferative cell divides, both daughter cells are proliferative cells, and a proliferative cell has a chance to undergo differentiation at any given instance.

It is clear that verification of the cell lineage in an epithelium requires quantitative experimental analysis and comparison with theoretical models. In this *article* we propose a minimal model for stratified epithelia, and we study how different differentiation mechanisms and cell–cell interactions affect the steady state properties. Besides providing a connection between the model parameters and the distribution of cells in the tissue steady state, the main findings of this study include the following. First, we find that there is no stratified steady state when there are only short-range interactions between the cells. This means that interactions which has a range large compared to cell size such as those mediated by diffusing morphogen molecules or mechanical stress are necessary for a tissue to maintain a stratified homeostasis state. Second, comparing to the model in which cell differentiation happens only during cell division, the model which assumes that cell differentiation is decoupled from cell division is able to produce more stratified tissues. These results invite future experiments to check if indeed in most stratified epithelia cell differentiation is decoupled from cell division. Next, when short-range interactions are present, there is a parameter regime where two tissue steady states coexist. In this region one of the solution has a high degree of stratification, it resembles a healthy mature tissue. Another solution is not highly stratified. This solution could be related to some anomalies of tissue morphology. This result suggests an interesting role played by short-range interactions in tissue morphogenesis.

2. Model

Consider a tissue that sits on a rigid stroma. The stroma is located on the xy plane, and grows into $z > 0$ region with a free apical surface (figure 1). For simplicity, we assume that the cell lineage of the tissue is composed of only two types of cells, proliferative and differentiated cells. If the differentiation of proliferative cells takes place only during cell division, the evolution of the density of proliferative and differentiated cells can be described by the following continuity equations

$$\partial_t \rho_P + \partial_l(\rho_P v_l) = r_P(2p_S - 1)\rho_P, \tag{1}$$

$$\partial_t \rho_D + \partial_l(\rho_D v_l) = 2r_P(1 - p_S)\rho_P - r_D\rho_D, \tag{2}$$

where $0 \leqslant p_S \leqslant 1$ is the self-renewal probability of the proliferative cells, $\rho_{P(D)}$ is the number density of the proliferative (differentiated) cells, and v_l is the lth component of the velocity field ($l \in \{x, y, z\}$). We have used Einstein summation convention therefore repeated indices are summed. r_P and r_D are the proliferation rate and the apoptosis rate, respectively.

On the other hand, if cell differentiation is decoupled from cell division, after a cell division event both daughter cells are proliferative cells. At any instance, every differentiated cell has a rate of apoptosis r_D, and every proliferative cell has a transition rate r_T to become a differentiated cell by cell differentiation. In this model the continuity equations for cell densities are

$$\partial_t \rho_P + \partial_l(\rho_P v_l) = r_P\rho_P - r_T\rho_P, \tag{3}$$

$$\partial_t \rho_D + \partial_l(\rho_D v_l) = r_T\rho_P - r_D\rho_D. \tag{4}$$

It is easy to see that replacing $2r_P(1 - p_S)$ by r_T, equations (1), (2) can be mapped to equations (3), (4). However, the mapping only maps the cell lineage model described by equations (1), (2) into the parameter space of the cell lineage model described by equations (3), (4) where

$$r_T \leqslant 2r_P. \tag{5}$$

From this result we know that substituting $r_T = 2r_P(1 - p_S)$ into the results of the analysis of the cell lineage model with decoupled cell differentiation and division, one obtains the results for the other cell linear model. Therefore from now on we use the notation in the model described by equations (3), (4), and when necessary we show the result of the other cell lineage model by a change of parameter. Note that the cell lineage model with coupled cell differentiation and cell division covers a smaller parameter range than the cell lineage model described by equations (3), (4) because $2r_P(1 - p_S) \leqslant 2r_P$, but there is no restriction on the magnitude of r_T when cell differentiation is decoupled from cell proliferation. Assuming incompressibility and introducing local proliferative cell proportion $\Lambda_P \equiv \rho_P/(\rho_P + \rho_D)$, equations (3), (4) can be rewritten as

$$D_t\Lambda_P = [r_D + r_P - r_T - (r_D + r_P)\Lambda_P]\Lambda_P, \tag{6}$$

$$\partial_l v_l = (r_D + r_P)\Lambda_P - r_D \equiv k_p, \tag{7}$$

where $D_t \equiv \partial_t + v_l \partial_l$ is the material derivative operator, and k_p is the net cell proliferation rate. For normal incompressible fluid the continuity equation is $\partial_l v_l = 0$, thus in our model the tissue behaves as a fluid with a source term that depends on the scalar field Λ_P. Notice that for a mature epithelium, k_p is a decreasing function of z. Since proliferative cells are mainly located close to the basal surface, $k_p > 0$ at small z and $k_p(z) < 0$ as one approaches the apical surface due to apoptoses of the differentiated cells. Furthermore, at $z = 0$ the usual no-slip boundary condition $v_l = 0$ holds.

To have robust and stable tissue developing pattern, cell division, differentiation, and apoptosis should be regulated by either short-range interaction through cell–cell direct contact, or interaction mediated by mechanical stress or diffusive signaling molecules called morphogen that is produced and degraded by cells in the tissue or the environment [14]. An example of the morphogen in the olfactory epithelia are the TGFβ family proteins. These protein molecules are produced by the cells in the olfactory epithelium, and they diffuse in the tissue over distances large compared to the size of a cell to regulate cell division and differentiation through a positive feedback mechanism [15]. This means that r_D, r_P and r_T are functions of Λ_P and another field M. The dependence on Λ_P characterizes how these rates are affected by the neighboring cells, the dependence on M characterizes how these rates are affected by mechanical stress or morphogen concentration.

To study the time evolution of the tissue, the dynamics of the morphogen density needs to be specified, and the mechanical properties of the tissue need to be taken into account [16]. However, in this work we focus on the steady state, therefore certain details of the complete model do not affect our study. For example, we know that the spatial distributions of the morphogen and the mechanical stress do not change with time. This means that the steady state mechanical stress and morphogen density are both functions of z. Therefore the evolution equations for the morphogen and the mechanical stress are not important in the study of tissue steady state, we can simply assume that in the steady state $M = M^*(z)$. In general $M^*(z)$ is a smooth function of z. However, to have a stratified steady state, the response of the cells in the tissue to morphogen concentration or mechanical stress often show cooperativity such that the differentiation and proliferation rates of the proliferative cells change abruptly when M exceeds (or decreases below) some threshold magnitude M_S [6]. Let h_P be the magnitude of z where $M^*(z) = M_S$. It is clear that the proportion of the proliferative cells should change dramatically around $z = h_P$, and h_P is the characteristic length of the tissue related to the thickness of the niche of the proliferative cells. Furthermore, in the case when r_D is a constant, one can choose r_D^{-1} as the unit time. In more general situation, since the time derivatives of the cell densities vanish in the steady state, we can still divide equations (6), (7) by r_D and redefine $\hat{r}_T \equiv r_T/r_D$ and $\hat{r}_P \equiv r_P/r_D$ to simplify the analysis. Consequently, in the steady state the two relevant dimensionless rates are

$$\hat{r}_{T(P)} = \hat{r}_{T(P)}(M^*(z),\, \Lambda_P^*) = \hat{r}_{T(P)}(z,\, \Lambda_P^*). \tag{8}$$

Symbols with superscript '*' denote the steady state magnitudes of the corresponding physical quantities. The effect of morphogen density and mechanical stress on the cell division and differentiation rates is now manifested in the z-dependence of $\hat{r}_{T(P)}$.

In the steady state the only non-vanishing component of the velocity field is v_z, and all physical quantities only depend on z. By choosing h_P as the unit length, in the steady state equations (6), (7) can be cast into the following dimensionless form

$$\tilde{v}_z^* \partial_{\tilde{z}} \Lambda_P^* = [1 + \hat{r}_P - \hat{r}_T - (1 + \hat{r}_P)\Lambda_P^*]\Lambda_P^*, \tag{9}$$

$$\partial_{\tilde{z}} \tilde{v}_z^* = (1 + \hat{r}_P)\Lambda_P^* - 1 \equiv \hat{k}_p^*, \tag{10}$$

where $\tilde{v}_z \equiv v_z/(r_D h_P)$, $\tilde{z} \equiv z/h_P$ and $\hat{k}_p^* \equiv k_p^*/r_D$. One can solve equations (9), (10) for given regulation functions $\hat{r}_{T(P)}(\tilde{z},\, \Lambda_P^*)$.

To determine the steady state tissue height, note that when $\tilde{z}$ is small, the tissue should be mainly occupied by the proliferative cells. This makes $\hat{k}_p^*(0) > 0$, and the daughter cells that are produced after cell proliferation should gradually migrate upwards, differentiate into differentiated cells, and keep moving towards the apical surface until they undergo apoptosis. This makes $\tilde{v}_z^* > 0$ for $0 < \tilde{z} < \tilde{H}^*$, where $\tilde{H}^* \equiv H^*/h_P$ is the dimensionless steady state tissue height. We call a solution with these properties a stratified steady state. Since $\tilde{v}_z^*(0) = \tilde{v}_z^*(\tilde{H}^*) = 0$, equation (10) leads to

$$\int_0^{\tilde{H}^*} [(1 + \tilde{r}_P)\Lambda_P^* - 1]\mathrm{d}\tilde{z} = \int_0^{\tilde{H}^*} \hat{k}_p^*\, \mathrm{d}\tilde{z} = 0. \tag{11}$$

From this equation, the steady state tissue height $\tilde{H}^*$ can be solved. Equation (11) simply describes the balance of total cell production and cell death events in the steady state. Equation (11) also implies that $\hat{k}_p^*(\tilde{H}^*) < 0$, that is, as one moves towards the apical surface, the density of differentiated cells becomes higher, and the net cell proliferation rate turns negative due to cell apoptosis events.

3. Discussions

3.1. Condition for the existence of stratified steady state

We have introduced equations (9), (10), two coupled nonlinear ordinary differential equations for Λ_P^* and $\tilde{v}_z^*$. Naively, besides $\tilde{v}_z^*(0) = 0$, once the boundary conditions for Λ_P^* are given, one should be able to integrate these equations and obtain the steady state solution. From equation (9)

$$\partial_{\tilde{z}}\Lambda_P^*(0) = \lim_{\tilde{z}\to 0} \frac{[1 + \hat{r}_P - \hat{r}_T - (1 + \hat{r}_P)\Lambda_P^*]\Lambda_P^*}{\tilde{v}_z^*} \tag{12}$$

and $\tilde{v}_z^*(0) = 0$, for the limit on the right hand side of equation (12) to exist, the numerator on the right hand side must vanish. This fixes the magnitude of the proportion of proliferative cells at $\tilde{z} = 0$ to

$$\Lambda_P^*(0) = \left(\frac{1 + \hat{r}_P - \hat{r}_T}{1 + \hat{r}_P}\right)_{\tilde{z}=0}. \tag{13}$$

Using L'Hôpital's rule, noticing that $\frac{d\hat{r}_{P,T}}{d\tilde{z}} = \partial_{\tilde{z}}\hat{r}_{P,T} + (\partial_{\Lambda_P^*}\hat{r}_{P,T})\partial_{\tilde{z}}\Lambda_P^*$, and using equations (9), (10), (12), (13), one can determine $\partial_{\tilde{z}}\Lambda_P^*(0)$,

$$\partial_{\tilde{z}}\Lambda_P^*(0) = \left(\frac{\Lambda_P^*[(1 - \Lambda_P^*)\partial_{\tilde{z}}\hat{r}_P - \partial_{\tilde{z}}\hat{r}_T]}{2(1 + \hat{r}_P)\Lambda_P^* - 1 - \Lambda_P^*[(1 - \Lambda_P^*)\partial_{\Lambda_P^*}\hat{r}_P - \partial_{\Lambda_P^*}\hat{r}_T]}\right)_{\tilde{z}=0}. \tag{14}$$

In the special case where cell differentiation and cell division rates are not affected by morphogen or stress mediated interactions, $\partial_{\tilde{z}}\hat{r}_T$ and $\partial_{\tilde{z}}\hat{r}_P$ both vanish and $\Lambda_P^*(0)$ is a fixed point of equation (9). As a result Λ_P^* is a constant throughout the tissue, and $\partial_{\tilde{z}}\tilde{v}_{\tilde{z}}^*$ is also a constant. This means that there is no stratified steady state, and we find that for our simple model to have stratified steady states, interactions mediated by morphogen or mechanical stress that can provide the spatial information to the cells are essential. Note that as long as the steady state tissue Λ_P^* satisfies an equation with advection like equation (9) and no-slip condition at the basal surface, we always need morphogen or stress mediated interactions for tissue stratified steady state to exist. Our simple model has revealed a quite general result.

3.2. Minimal model without short-range interactions

Since morphogen or stress mediated interactions are essential for a tissue to have a stratified steady state, we consider a minimal model in which such an interaction provides the information for a cell to adjust its differentiation rate. In this minimal model, short-range interactions are neglected and proliferation rate is assumed to be a constant. This is the simplest model which has a stratified steady state. A slightly more general model in which $\hat{r}_P$ is also a function of $\tilde{z}$ shows similar results. This is discussed in the appendix.

To take into account the cooperativity of the response of the proliferative cells to the magnitude of M, the regulation function $\hat{r}_T$ is chosen to be a Hill function of $\tilde{z}$,

$$\begin{cases} \hat{r}_P = \hat{r}_P^{(0)}, \\ \hat{r}_T = \dfrac{\tilde{z}^n}{1 + \tilde{z}^n}\hat{r}_T^{(0)}, \end{cases} \tag{15}$$

where $\hat{r}_P^{(0)}$ and $\hat{r}_T^{(0)}$ are two positive constants, and n is the Hill coefficient which characterizes the degree of cooperativity in the response of $\hat{r}_T$ to the smoother distribution of morphogen or mechanical stress. As n increases the corresponding Hill function becomes steeper at $\tilde{z} = 1$. Since $\hat{r}_T(\tilde{z}) \to 0$ as $\tilde{z} \to 0$, equations (9) and (13) give $\Lambda_P^*(\tilde{z}) \to 1$ for $\tilde{z} < 1$, i.e., the proliferative cells have a niche in the basal region with a characteristic height h_P. Intuitively large n is needed for a tissue to achieve a highly stratified homeostasis state.

From equations (13)–(15), one obtains

$$\Lambda_P^*(0) = 1, \text{ and } \partial_{\tilde{z}}\Lambda_P^*(0) = \frac{-\beta(0)}{1 + 2\hat{r}_P^{(0)}}, \tag{16}$$

where

$$\beta(\tilde{z}) = -2n\hat{r}_T^{(0)}\frac{\tilde{z}^{n-1}}{(1 + \tilde{z}^n)^2}. \tag{17}$$

By numerically integrating equations (9), (10), and solving $\Lambda_P^*(\tilde{z})$ with $\tilde{H}^*$ determined by equation (11), the steady state of the tissue can be solved for given $\hat{r}_T^{(0)}$, $\hat{r}_P^{(0)}$, and n. On the other hand, for sufficiently strong cooperativity, one can take $n \to \infty$ and solve equations (9), (10), and (15) analytically. As discussed in equation (A.5) steady state solution with vanishing Λ_P^* at the apical surface exists when $\hat{r}_T^{(0)} > 1 + \hat{r}_P^{(0)}$, and the steady state solutions of Λ_p^* and $\tilde{v}_z^*$ in the limit $n \to \infty$ are

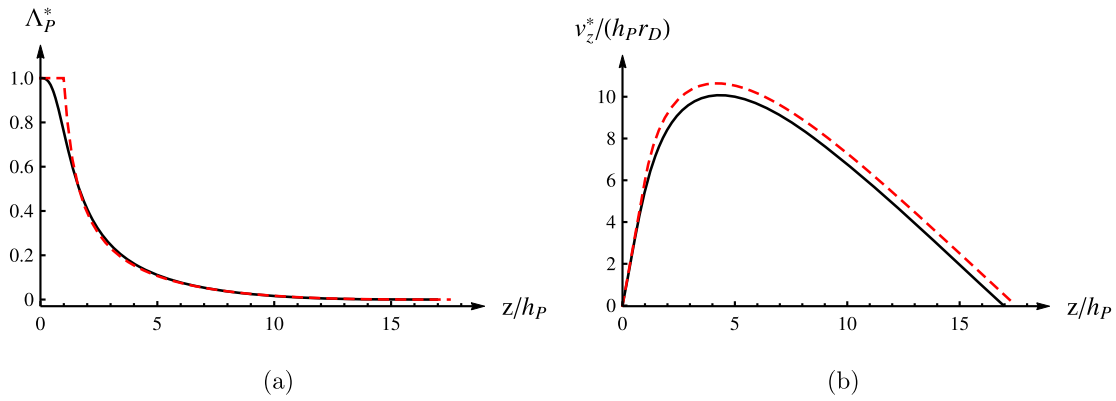

Figure 3. Typical stratified steady state profiles of proliferative cell proportion (Λ_P^*) and flow speed (v_z^*) in our model. The solid black curve is from the numerical solutions of equations (9), (10), and (15) with $n = 3$, $\hat{r}_P^{(0)} = 6$, and $\hat{r}_T^{(0)} = 10$. The dashed red curves are from the analytical solutions at $n \to \infty$ (equations (18)–(20)) with the same $\hat{r}_P^{(0)}$ and $\hat{r}_T^{(0)}$.

$$\Lambda_P^*(\tilde{z}) = \begin{cases} 1 & , \tilde{z} < 1 \\ \dfrac{\hat{r}_T^{(0)} - 1 - \hat{r}_P^{(0)}}{\hat{r}_T^{(0)} \exp[(\hat{r}_T^{(0)} - 1 - \hat{r}_P^{(0)})\tilde{t}(\tilde{z})] - 1 - \hat{r}_P^{(0)}} & , \tilde{z} \geqslant 1, \end{cases} \tag{18}$$

and

$$\tilde{v}_z^*(\tilde{z}) = \begin{cases} \hat{r}_P^{(0)}\tilde{z} & , \tilde{z} < 1 \\ \dfrac{\hat{r}_P^{(0)}}{\hat{r}_T^{(0)} - 1 - \hat{r}_P^{(0)}} \{\hat{r}_T^{(0)} \exp[-\tilde{t}(\tilde{z})] - (1 + \hat{r}_P^{(0)}) \exp[(\hat{r}_P^{(0)} - \hat{r}_T^{(0)})\tilde{t}(\tilde{z})]\} & , \tilde{z} \geqslant 1, \end{cases} \tag{19}$$

where $\tilde{t}(\tilde{z})$ is the inverse of the function

$$\tilde{z}(\tilde{t}) = 1 + \frac{\hat{r}_P^{(0)}[\hat{r}_T^{(0)}(\hat{r}_T^{(0)} - \hat{r}_P^{(0)})[-1 + \exp(-\tilde{t})] - (1 + \hat{r}_P^{(0)})(-1 + \exp[-(\hat{r}_T^{(0)} - \hat{r}_P^{(0)})\tilde{t}])]}{(\hat{r}_T^{(0)} - \hat{r}_P^{(0)})(1 + \hat{r}_P^{(0)} - \hat{r}_T^{(0)})}. \tag{20}$$

For comparison, figure 3 shows the proportion of proliferative cells and flow field v_z^* for solutions with $n = 3$ and $n \to \infty$ for a typical choice of parameters. It clearly shows that a tissue can have good stratification even when n is as small as 3. Since stratified homeostasis state can already be achieved with moderate n, we further check how $\Lambda_P^*(z)$, proportion of the proliferative cells in the homeostasis state, varies with n, $\hat{r}_P^{(0)}$, and $\hat{r}_T^{(0)}$ in figure 4. First, figure 4(a) shows that when $n = 1$, Λ_P^* decreases rapidly even for $\tilde{z} < 1$, indicating the absence of a clear proliferative cell niche. On the other hand, for $n \geqslant 3$ the qualitative features of Λ_P^* are insensitive to n and a proliferative cell niche can be identified. Figures 4(b) and (c) show that although Λ_P^* is insensitive to n for $n \geqslant 3$, it is sensitive to both $\hat{r}_P^{(0)}$ and $\hat{r}_T^{(0)}$. As $\hat{r}_P^{(0)}$ increases, cell division rate increases, as a result the tissue needs to have more differentiated cells in the steady state to have equal number of cell apoptosis events per unit time to balance cell division, and $\tilde{H}^*$ increases. On the other hand, increasing $\hat{r}_T^{(0)}$ makes cell differentiate faster, this lowers the number of proliferative cells, leads to smaller $\tilde{H}^*$, and the tissue shows sharper transition between the proliferative cell niche and the apical differentiated region.

The analytical expression in the $n \to \infty$ limit (equations (18)–(20)) makes it convenient to discuss the following interesting quantities which characterize a tissue steady state.

- We first discuss the dimensionless steady state tissue height in the limit $n \to \infty$ obtained from equations (11) and (18),

$$\tilde{H}^* = \frac{\hat{r}_T^{(0)}(1 + \hat{r}_P^{(0)})}{\hat{r}_T^{(0)} - \hat{r}_P^{(0)}}. \tag{21}$$

  $1/\tilde{H}^* = h_P/H^*$ gives us the relative size of the proliferative cell niche in the tissue. For a mature stratified epithelium that functions normally $1/\tilde{H}^*$ should be sufficiently small. For example, experiment on olfactory epithelium reported that $\tilde{H}^* \approx 10$ [17]. In figure 5(a) we plot $\tilde{H}^*$ versus $\hat{r}_P^{(0)}$ for several choices of $\hat{r}_T^{(0)}$ to compare equation (21) with numerical solution for $n = 3$, and we find that the difference is small. For all curves, $\tilde{H}^*$ increases with $\hat{r}_P^{(0)}$ and decreases with $\hat{r}_T^{(0)}$. The condition $\tilde{H}^* \gg 1$ can be satisfied for $\hat{r}_P^{(0)}$ large compared to unity.

- To describe the thickness of the transition region between the proliferative cell niche and the differentiated cell niche, we introduce transition length $h_T \equiv h_c - h_P$. h_c is the position where the proportion of proliferative

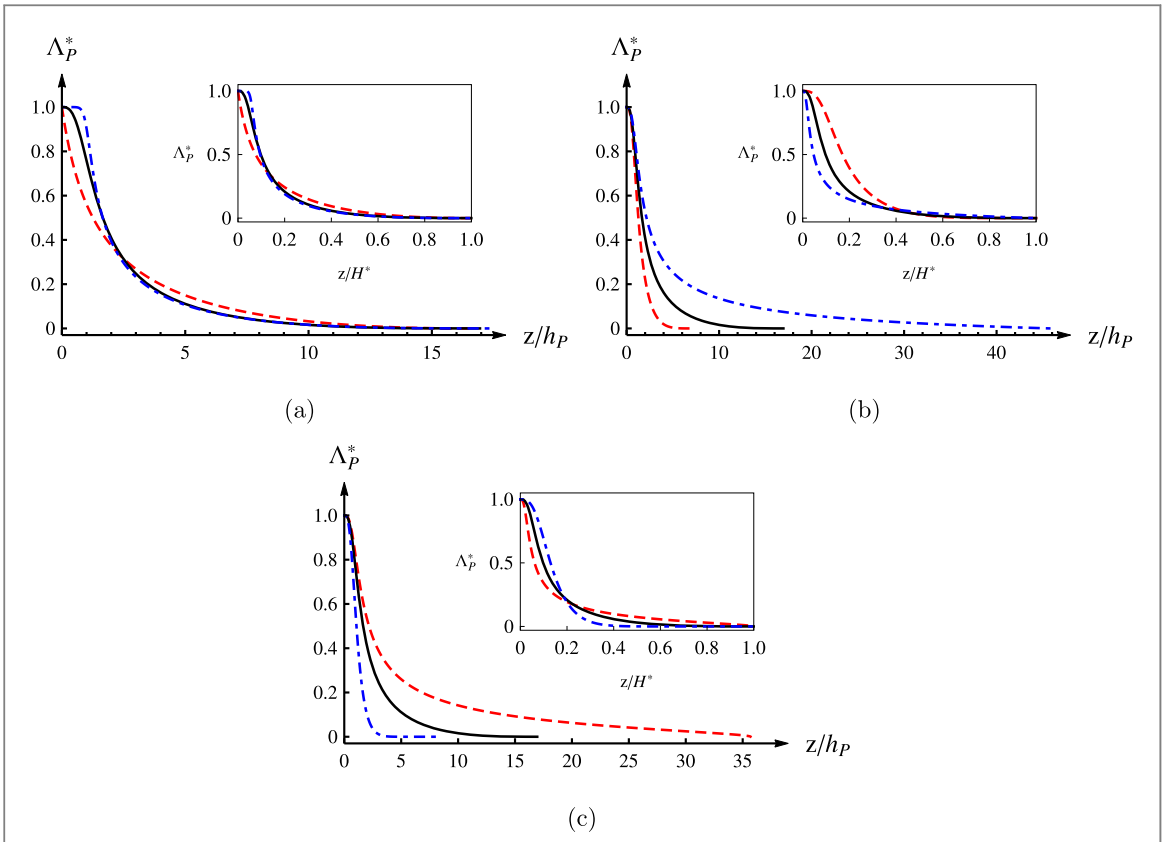

Figure 4. Λ_P^*, proportion of proliferative cells at height z in a tissue with no short-range interactions. The parameters are the same as those in figure 3 for solid black lines, but in (a) $n = 1$ for dashed red curve and $n = 10$ for dot-dashed blue curve, in (b) $\hat{r}_P^{(0)} = 4$ for dashed red curve and $\hat{r}_P^{(0)} = 8$ for dot-dashed blue curve, in (c) $\hat{r}_T^{(0)} = 7.5$ for dashed red curve and $\hat{r}_T^{(0)} = 20$ for dot-dashed blue curve. The insets show Λ_P^* versus z/H^* to illustrate the degree of stratification for different parameters. Some characteristics of these curves as functions of $\hat{r}_P^{(0)}$, $\hat{r}_T^{(0)}$ and n are plotted in figure 5.

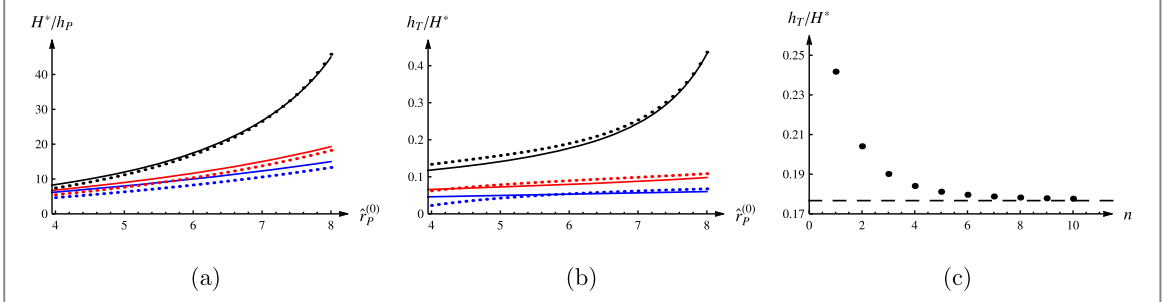

Figure 5. (a) Tissue height H^* and (b) transition length h_T versus the characteristic cell proliferation rate $\hat{r}_P^{(0)}$ for different characteristic cell differentiation rate $\hat{r}_T^{(0)}$ in a tissue with no short-range interactions. The regulation functions are given in equation (15). The two (black) curves on the top have $\hat{r}_T^{(0)} = 10$, the two (red) curves in the middle have $\hat{r}_T^{(0)} = 15$, the two (blue) curves with lowest H^* have $\hat{r}_T^{(0)} = 20$. The dotted curves are numerical solutions for $n = 3$, the solid curves represent the analytical solution (equations (21), (22)) for $n \to \infty$. (c) h_T versus n for $\hat{r}_p^{(0)} = 6$ and $\hat{r}_T^{(0)} = 10$, the dashed line is h_T/H^* at $n \to \infty$.

cells Λ_P^* drops to $(\hat{r}_T^{(0)} - 1 - \hat{r}_P^{(0)}) / (\hat{r}_T^{(0)} e - 1 - \hat{r}_P^{(0)})$. When $n \to \infty$,

$$\frac{h_T}{H^*} = \frac{\hat{r}_P^{(0)}\{(1+\hat{r}_T^{(0)})\tilde{t}_c^{-1} - [\hat{r}_T^{(0)}(\hat{r}_T^{(0)} - \hat{r}_P^{(0)}) - (1+\hat{r}_P^{(0)})/e]\exp(-\tilde{t}_c)\}}{\hat{r}_T^{(0)}(1+\hat{r}_P^{(0)})(\hat{r}_T^{(0)} - 1 - \hat{r}_P^{(0)})}, \tag{22}$$

where $\tilde{t}_c \equiv (\hat{r}_T^{(0)} - 1 - \hat{r}_P^{(0)})^{-1}$. A sharp interface between the proliferative cell niche and the differentiated region corresponds to $h_T/H^* \ll 1$. Figure 5(b) shows that h_T/H^* decreases as $\hat{r}_P^{(0)}$ decreases and $\hat{r}_T^{(0)}$ increases. Figure 5(c) shows that h_T/H^* becomes close to its value at $n \to \infty$ for $n \geqslant 3$. This further confirms that highly stratified tissue can be achieved at reasonable n.

- The simplicity of this model makes it easy to be compared to experiments. For example, the overall proportion of proliferative cells $\bar{\Lambda}_P^*$ is

$$\bar{\Lambda}_P^* \equiv \frac{1}{\tilde{H}^*}\int_0^{\tilde{H}^*} \Lambda_P^*(\tilde{z})\, \mathrm{d}\tilde{z} = \frac{1}{1+\hat{r}_P^{(0)}}, \tag{23}$$

and $\bar{\Lambda}_P^*$ depends only on $\hat{r}_P^{(0)}$. Since the differentiated cells are functional cells in the tissue, in a mature stratified epithelium the magnitude of $\bar{\Lambda}_P^*$ should be much smaller than unity, this is achieved when $\hat{r}_P(0)$ is large compared to unity. By fitting equations (21) and (23) with experimental observations, we can deduce the corresponding magnitudes of $\hat{r}_P^{(0)}$ and $\hat{r}_T^{(0)}$.

The above results suggest that for a tissue steady state to have thickness $H^* \gg h_P$, transition length $h_T \ll H^*$, and overall proportion of proliferative cells $\bar{\Lambda}_P^* \ll 1$, the rates should satisfy

$$\hat{r}_T^{(0)} \gg \hat{r}_P^{(0)} \gg 1. \tag{24}$$

Notice that deducing the magnitudes of $\hat{r}_P^{(0)}$ and $\hat{r}_T^{(0)}$ from experimental data also provides a way to check if the cell lineage with coupled cell differentiation and cell division is a good candidate to describe the tissue under study. This is because, as pointed out in section 2, the cell lineage model with coupled cell differentiation and cell division only maps to the parameter region of the other cell lineage model where equation (5) is satisfied. If the experimental results suggest that $r_T > 2r_P$, then cell differentiation is very unlikely to be coupled to cell division. Since the transition length decreases as $\hat{r}_T^{(0)}$ increases (figure 5(b)), our analysis predicts that it is less likely for the cell lineage model with coupled cell differentiation and cell division to give a tissue with highly stratified steady state (for example, see dot-dashed blue curve in figure 4(b)).

As an example, let us apply our minimal model to the olfactory epithelium of mouse. It is known that $\bar{\Lambda}_P^* \sim$ 5%–10% in these tissues [18]. From equation (23) one finds that $\hat{r}_P^{(0)} \sim$ 10–20. On the other hand, to meet the experimental observed value $\tilde{H}^* \sim 10$ with $\hat{r}_P^{(0)}$ in this range, figure 4(a) suggests that one needs to have $\hat{r}_T^{(0)} \geqslant 20$. This means that it is likely that for mouse olfactory epithelium $\hat{r}_T^{(0)}$ is close to $2\hat{r}_P^{(0)}$, and $\hat{r}_T$ is close to $2\hat{r}_P$ when $\tilde{z} > 1$ if we assume $p_S \ll 1$ at $\tilde{z} > 1$. If indeed in mouse olfactory epithelium cell differentiation is coupled to cell division, then either evolution has driven the olfactory epithelium to maximize its stratification to the limit within the cell lineage model with coupled cell differentiation and cell division, or there exists some other mechanism not included in our minimal model which helps to give the experimentally observed composition of olfactory epithelium. For example, cell differentiation may be triggered by the dissociation of proliferative cells from the basal membrane [19, 20]. This mechanism, which is not included in our minimal model, may help making a tissue more stratified. Models with more details should be able to check if such mechanisms can be important in helping tissue stratification, or the olfactory epithelium has indeed evolved to maximize its stratification under the constraints provided in our minimal model.

3.3. Effect of short-range interactions

In principle, cell proliferation, differentiation, and apoptosis can also be affected by direct interactions between neighboring cells. To study the effects of such short-range interactions on tissue steady state, we include in $\hat{r}_P$ and $\hat{r}_T$ terms linear in Λ_P,

$$\hat{r}_P = \hat{r}_P^{(0)} + \hat{r}_P^{(1)}(1-\Lambda_P), \text{ and } \hat{r}_T = \frac{\tilde{z}^n}{1+\tilde{z}^n}\hat{r}_T^{(0)} + \hat{r}_T^{(1)}(1-\Lambda_P), \tag{25}$$

where $\hat{r}_P^{(1)}$ and $\hat{r}_T^{(1)}$ are constants, they can be positive or negative.

From equation (13), now it is possible to have two solutions for $\Lambda_P^*(0)$. One of the solutions always exists, it satisfies

$$\Lambda_P^*(0) = 1, \text{ and } \partial_{\tilde{z}}\Lambda_P^*(0) = \frac{-\beta(0)}{1+2\hat{r}_P^{(0)}-\hat{r}_T^{(1)}}, \tag{26}$$

where $\beta(\tilde{z})$ is defined in equation (17). Since equation (26) reduces to (16) as $\hat{r}_T^{(1)} \to 0$, we can identify it as the generalization of the solution we found in section 3.2. The other solution satisfies

$$\Lambda_P^*(0) = 1 + \frac{1+\hat{r}_P^{(0)}-\hat{r}_T^{(1)}}{\hat{r}_P^{(1)}}, \tag{27}$$

and

$$\partial_{\tilde{z}}\Lambda_P^*(0) = \frac{\hat{r}_P^{(1)}\beta(0)}{(1+\hat{r}_P^{(0)})^2 + \hat{r}_P^{(1)}(2+\hat{r}_P^{(0)}) - \hat{r}_T^{(1)}(3-2\hat{r}_T^{(1)}+2\hat{r}_P^{(1)}+3\hat{r}_P^{(0)})}. \tag{28}$$

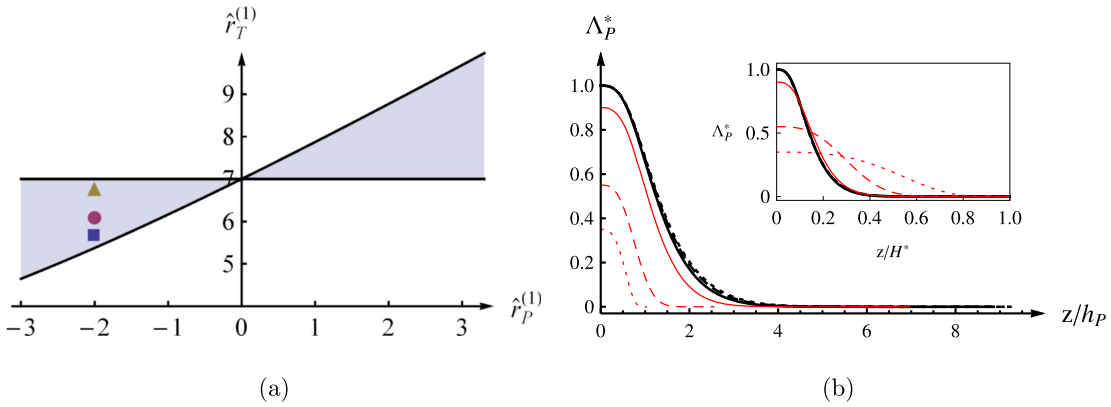

Figure 6. (a) Phase diagram for a tissue with both short-range interactions and interactions mediated by morphogen or mechanical stress. The regulation functions are given in equation (25). The parameters are $n = 3$, $\hat{r}_P^{(0)} = 6$, and $\hat{r}_T^{(0)} = 10$. The light purple regions are where two steady states coexist, in other regions there is only one steady state. The phase boundaries are given by equation (29). (b) Λ_P^* versus z/h_P for parameters given by the solid triangle, circle, and square in (a). $\hat{r}_P^{(1)} = -2$ for all curves, and $\hat{r}_T^{(1)} = 6.8$ for the solid curves, $\hat{r}_T^{(1)} = 6.1$ for the dashed curves, and $\hat{r}_T^{(1)} = 5.7$ for the dotted curves. The thick (black) curves are the original solutions which one also finds in a system with no short-range interactions, and the thin (red) curves represent the second solutions that only exist in the presence of short-range interactions. The inset shows the corresponding Λ_P^* versus z/H^* to illustrate the degree of stratification for different parameter choices.

For this solution to satisfy $0 \leqslant \Lambda_P^*(0) \leqslant 1$ and $\hat{k}_p^*(\tilde{z} = 0) \equiv [(1 + \hat{r}_P)\Lambda_P^* - 1]_{\tilde{z}\to 0} > 0$, the following conditions need to be satisfied,

$$\hat{r}_P^{(1)}(1 + \hat{r}_P^{(0)}) \leqslant \hat{r}_P^{(1)}\hat{r}_T^{(1)} < \hat{r}_P^{(1)}\left(\frac{1 + \hat{r}_P^{(0)} + \hat{r}_P^{(1)}}{2} + \sqrt{\left(\frac{1 + \hat{r}_P^{(0)} + \hat{r}_P^{(1)}}{2}\right)^2 - \hat{r}_P^{(1)}}\right), \tag{29}$$

The first inequality becomes an equality when $\Lambda_P^*(0) = 1$, and the second inequality holds when $\hat{k}_p^*(\tilde{z} = 0) > 0$. In the following we refer the solution that satisfies the boundary conditions listed in equation (26) as the 'original solution', and the other one that satisfies equations (27), (28) as the 'second solution'. From equation (29) the parameter regime where two steady state solutions coexist can be plotted, this is presented in figure 6(a). It is clear that for given $\hat{r}_P^{(1)}$, there is a window of $\hat{r}_T^{(1)}$ where the tissue has two steady states.

To understand the physical origin of the second solution of the steady state, it is instructive to consider the special case where $\hat{r}_T^{(0)} = 0$. From equation (25), in this case both $\hat{r}_P$ and $\hat{r}_T$ have no explicit dependence on $\tilde{z}$, i.e., the dimensionless cell differentiation and cell division rates are completely controlled by short-range interactions. According to our discussion in section 3.1, the steady state solution in this case satisfies $\tilde{v}_z^* = 0$ and $\hat{k}_p^* = 0$ everywhere. Furthermore, direct solving equations (9), (10) leads to the steady state solution for Λ_P^*,

$$\Lambda_P^*|_{\hat{r}_T^{(0)}=0} = 1 - \frac{\hat{r}_P^{(0)}}{\hat{r}_T^{(1)} - \hat{r}_T^{(1)}},$$

where $\hat{r}_T^{(1)}$ has to satisfy the following solvability condition

$$\hat{r}_T^{(1)} = \left(\frac{1 + \hat{r}_P^{(0)} + \hat{r}_P^{(1)}}{2} + \sqrt{\left(\frac{1 + \hat{r}_P^{(0)} + \hat{r}_P^{(1)}}{2}\right)^2 - \hat{r}_P^{(1)}}\right). \tag{30}$$

Note that this solvability condition is nothing but the condition $\hat{k}_p^* = 0$, therefore the right hand side of equation (30) also appears in the second inequality of equation (29). Now we can use this special case to help us to clarify the physical mechanism that leads to the second solution. In general, short-range interactions in our model can be viewed as a mechanism that drives the tissue towards a homogeneous steady state, only the presence of interactions mediated by morphogen or mechanical stress can help the tissue to stabilize a stratified steady state. Therefore in the presence of both short-range interaction and interaction mediated by morphogen or mechanical stress, there is a range of parameters where the competition of these two mechanisms gives the tissue two steady states. It will become clear that one of these solutions resembles the solution provided by the minimal model without short-range interactions, and the second solution is significantly influenced by the short-range interactions.

To illustrate the differences between the original solution and the second solution, the composition of the tissue for three different $\hat{r}_T^{(1)}$'s in the two-state region with negative $\hat{r}_P^{(1)}$ is presented in figure 6(b). According to equation (29), in this case the second steady state shows up as $\hat{r}_T^{(1)}$ drops below $1 + \hat{r}_P^{(0)}$. When $\hat{r}_T^{(1)}$ is not much

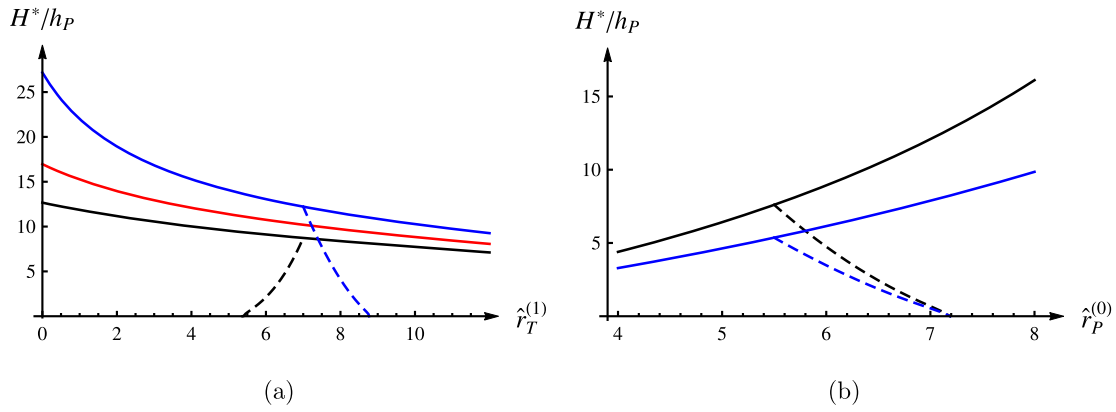

Figure 7. The bifurcation of steady state tissue height due to short-range interactions. The regulation functions are given in equation (25). (a) H^*/h_P versus $\hat{r}_T^{(1)}$, (b) H^*/h_P versus $\hat{r}_P^{(0)}$. These are taken from the numerical solutions for Hill parameter $n = 3$. In (a) $\hat{r}_P^{(0)} = 6$, $\hat{r}_T^{(0)} = 10$, and $\hat{r}_P^{(1)} = -2$ (solid black curve, it has the smallest H^*/h_P), 0 (solid red curve, the curve in the middle), and 2 (solid blue curve, it has the largest H^*/h_P). In (b) $\hat{r}_P^{(1)} = -2$, $\hat{r}_T^{(1)} = 6.5$, and $\hat{r}_T^{(0)} = 10$ (solid black curve, it has greater H^*/h_P) and 20 (solid blue curve, it has smaller H^*/h_P). The corresponding dashed curves in the figures are the new steady states created by short-range interactions.

smaller than $1 + \hat{r}_P^{(0)}$ the second solution is not very different from the original solution. It still gives pretty good stratification because the magnitude of $\Lambda_P^*(0)$ is close to one. However, as $\hat{r}_T^{(1)}$ decreases, the shape of Λ_P^* for the second solution becomes less stratified until $\hat{r}_T^{(1)}$ satisfies equation (30), where $\hat{k}_p^* = \hat{v}_z^* = 0$ everywhere and a stratified steady state with nonzero finite thickness no longer exists. The tendency that the second solution has decreasing tissue stratification as $\hat{r}_T^{(1)}$ decreases is clearly illustrated in the inset of figure 6(b). On the other hand, the original solution shows almost no dependence on the magnitude of $\hat{r}_T^{(1)}$, indicating that this solution is mostly shaped by the interaction mediated by morphogen or mechanical stress.

Figure 7 shows tissue thickness $\tilde{H}^*$ versus $\hat{r}_T^{(1)}$ and $\hat{r}_P^{(0)}$. For given $\hat{r}_P^{(1)}$, the original solution bifurcates into two solutions at $\hat{r}_T^{(1)} = 1 + \hat{r}_P^{(0)}$, and the second solution is very sensitive to $\hat{r}_T^{(1)}$ and $\hat{r}_P^{(0)}$. Especially, figure 7(a) shows that after the bifurcation occurs the tissue height of the second solution starts to deviate from the original solution. In this regime $\tilde{H}^*$ of the second solution decreases quickly as $\hat{r}_T^{(1)}$ increases (decreases) when $\hat{r}_P^{(1)} > (<) 0$. Eventually the thickness of the tissue for the second solution vanishes at the value of $\hat{r}_T^{(1)}$ which has $\hat{k}_p^* = 0$. Figure 7(b) shows that for fixed $\hat{r}_P^{(1)} (< 0)$ and $\hat{r}_T^{(1)}$ the tissue can enter the two-state regime by varying $\hat{r}_P^{(0)}$. Again, the tissue thickness of the original solution varies smoothly as $\hat{r}_P^{(0)}$ changes, and the tissue thickness of the second solution decreases as $\hat{r}_P^{(0)}$ further increases until $\tilde{H}^*$ becomes zero due to vanishing $\hat{k}_p^*$.

3.4. Possible extensions of our model

3.4.1. On the effect of necrosis

Besides apoptosis, necrosis also happens frequently in biological tissues [22]. It is interesting to discuss how necrosis changes the results of our model. Note that the cell death rate r_D in our model is, in general, not independent of cell density. This means that in our model r_D can include contribution from both apoptosis and necrosis. In the steady state one can still introduce $\hat{r}_T = r_T/r_D$ and $\hat{r}_P = r_P/r_D$. Since necrosis events per unit time per unit volume does not have to be proportional to local cell density, this means that in the presence of necrosis $\hat{r}_T$ and $\hat{r}_P$ should depend on Λ_P. Thus in the language of section 3.3, a tissue with significant contribution from cell necrosis is a tissue with 'short-range interactions'.

The main point is that the analysis presented for our model still applies when necrosis is considered, but the interpretation of the results should be slightly modified. For example, the 'short-range interactions' that affect $\hat{r}_P = r_P/r_D$ and $\hat{r}_T = r_T/r_D$ now include contribution from necrosis. Therefore it is possible for necrosis to induce the second solution of the steady state. This means that in a model that include detailed description of necrosis, it is possible to find a link between the less stratified second solution and cell necrosis.

3.4.2. Possible extension of our model to other epithelia

Although our model describes a stratified epithelium growing in the vertical direction, it is possible to extend this model to describe a monolayer epithelium with vertical progress of cells, for example an intestinal crypt [23]. The stem cells in an intestinal crypt are located at the base. As cells divide new daughter cells move upwards and gradually differentiate, therefore the cells close to the tips are differentiated cells. This tissue geometry is quite parallel to the vertical arrangement of the stratified epithelium considered in our model. Note that in the steady

state the cells at the bottom and the tip all have zero velocity due to the symmetry of the crypt, therefore the apparent difference in the shape of a stratified epithelium and an intestinal crypt does not give them different flow field boundary conditions. On the other hand, although the vertical progress of cells makes an intestinal crypt a good analogy to a stratified epithelium, direct applying our model to this epithelium does not take the variation of horizontal perimeter of an intestinal crypt into account. A model which takes this difference into account should only mildly modify our model results quantitatively. Another difference comes from the fact that the epithelium of an intestinal crypt is a monolayer, therefore every cell in the epithelium is in contact with the basal membrane. It is thus possible for the basal membrane to directly interact with all the cells in the epithelium. Therefore when applying our model to the intestinal crypt epithelium the interactions that lead to the z-dependence of $\hat{r}_P$ and $\hat{r}_T$ can also be induced by direct contact between the tissue and the basal membrane, and morphogen or stress mediated interactions are not the only possibilities anymore.

4. Conclusion

It has been known for a long time that the homeostasis of a stratified epithelium is controlled by both short-range interactions and interactions mediated by morphogen or mechanical stress. However, the roles played by these interactions are still not well-understood. In this work we try to answer these questions by building the simplest models and studying the distribution of proliferative cells in the steady states.

First, we find that signaling from morphogen or mechanical stress that regulates cell lineage dynamics is necessary for a tissue to have a stratified steady state. In general, the evolution of a tissue toward the steady state depends on many details that are not included in our model, but in our study the necessity of morphogen or mechanical stress mediated interactions for the existence of stratified steady state comes from the advection term in the evolution equation for Λ_P^* and zero tissue flow field at the basal surface. These are quite general features, thus in general for a stratified epithelium to have a steady state, such interactions are necessary. Notice that our study focuses on the vertical direction, and we have assumed homogeneous distribution in the horizontal directions. Therefore it is possible that the homogeneity in the horizontal directions can be established by short-range interactions. Furthermore, it is also important to point out that the necessity of interaction mediated by morphogen or mechanical stress for the stratified steady state holds only when cell differentiation induced by the loss of adhesion to the basal membrane is not important to the tissue.

Further study on the steady state shows that for a broad range of parameters the thickness of the proliferative cell niche is small. On the other hand, the thickness of the transition region between the proliferative cell niche and the differentiated cell region is small when the characteristic cell differentiation rate $\hat{r}_T^{(0)}$ is large. This in turn indicates that, compared to the cell lineage model in which cell differentiation is coupled to cell division, the other cell lineage model is able to maintain a more stratified tissue. One should note that this conclusion is purely physical, not biological. Although the cell lineage model with decoupled cell differentiation and cell division can maintain a more stratified tissue, whether a tissue's degree of stratification needs to be in a range outside of the reach of a tissue with coupled cell differentiation and cell division to make the tissue biologically functional is another question. As recent studies on various neural tubes [21] show, current experimental data supports cell lineages with coupled cell differentiation and cell division in these tissues. It is therefore interesting for future studies to see if the other cell lineage model is common in stratified epithelium.

When short-range interactions are included in our model, we find that it is possible for a tissue to have two steady states. One of these steady states looks very similar to the steady state of a tissue without short-range interaction. It can be highly stratified for a wide range of parameters. On the other hand, the other steady state solution is usually less stratified, and has a smaller thickness. This solution seems to correspond to an unhealthy tissue. It seems that when the effect of the neighboring cells on a cell's differentiation and proliferation rate goes wrong, a tissue can become unhealthy. The questions related to how a tissue regulates its interactions to avoid such unhealthy state depend on more detailed models, and we leave this interesting issue to future studies.

Our simple model aims at asking general questions relating cell lineage and the steady state of a stratified epithelium. Indeed it has revealed the importance of interactions mediated by morphogen or mechanical stress and unexpected interesting effect of short-range interactions. Furthermore, it also provides a way to extract model parameters from experimental measurement of the ratio of proliferative cells in a tissue and the tissue thickness relative to the size of proliferative cell niche. As we also pointed out, our model can be extended to include necrosis, and the possibility that necrosis can induce the less stratified second steady state solution provides an interesting future research direction. With some caution our model can also be applied to describe the steady state of the intestinal crypt, as the vertical progress of the cells in its epithelium is similar to the movement of cells in a stratified epithelium. Finally, it will be interesting to include mechanical properties of the tissue in our model in the future. For example, the mechanical properties in a tissue should depend on the active

forces of the cells during cell division and cell apoptosis [24], therefore cell lineage and tissue mechanics should in general be related to each other, a model that include these relations will be a future work.

Acknowledgments

The authors would like to thank support from the Ministry of Science and Technology, Taiwan (grant number 105-2112-M-008-006-MY2) and NCTS. The authors are also grateful for stimulating discussions with J-F Joanny (ESPCI), and helpful discussions with C-M Chen (National Yang-Ming University, Taiwan).

Appendix. General model for tissues without short-range interaction

In this appendix, we derive the analytical solution of a general model which does not have short-range interactions. In this model, both proliferation rate and differentiation rate are position-dependent. Section 3.2 is a special case of this general model.

In this model, the dimensionless proliferation rate $\hat{r}_P$ and differentiation rate $\hat{r}_T$ are

$$\begin{aligned}\hat{r}_P &= \hat{r}_P^L + \frac{\tilde{z}^n}{1+\tilde{z}^n}(\hat{r}_P^H - \hat{r}_P^L),\\ \hat{r}_T &= \hat{r}_T^L + \frac{\tilde{z}^n}{1+\tilde{z}^n}(\hat{r}_T^H - \hat{r}_T^L),\end{aligned} \tag{A.1}$$

where the superscripts 'L' and 'H' denote the corresponding rates close to the basal membrane (L) and the apical surface (H). For simplicity the Hill coefficients of $\hat{r}_P$ and $\hat{r}_T$ are chosen to be the same. Since for $n \geqslant 3$ the steady state tissue properties depend very little on n, this simplification is expected not to change the results qualitatively. Furthermore, we will mostly discuss $n \to \infty$ limit in this appendix, in this limit there is no need to introduce two different Hill coefficients.

A few biological conditions need to be addressed, as they lead to some constraints on $\hat{r}_P^{H(L)}$ and $\hat{r}_T^{H(L)}$. First, there is a proliferative cell niche at small $\tilde{z}$ with $\Lambda_P^*(\tilde{z} \to 0) \to 1$. From equation (13), this condition leads to the choice

$$\hat{r}_T^L = 0. \tag{A.2}$$

Second, the net cell proliferation rate should be positive at small $\tilde{z}$, i.e., $\hat{k}_p^*(\tilde{z} \to 0) > 0$. From the definition of $\hat{k}_p^*$ in equation (10), this condition leads to

$$\hat{r}_P^L > 0. \tag{A.3}$$

Furthermore, the apical region should be occupied completely by differentiated cells, i.e. Λ_P^* vanishes as $\tilde{z} \to \tilde{H}^*$. From equations (9) and (A.1),

$$\Lambda_P^*(\tilde{z} \to \tilde{H}^*) = \begin{cases} \dfrac{1+\hat{r}_P^H - \hat{r}_T^H}{1+\hat{r}_P^H} & \hat{r}_T^H < 1 + \hat{r}_P^H \\ 0 & \hat{r}_T^H \geqslant 1 + \hat{r}_P^H, \end{cases} \tag{A.4}$$

Λ_P^* vanishes as $\tilde{z} \to \hat{H}^*$ requires

$$\hat{r}_T^H \geqslant 1 + \hat{r}_P^H. \tag{A.5}$$

Notice that the minimal model discussed in section 3.2 corresponds to $\hat{r}_T^H = \hat{r}_T^{(0)}$, $\hat{r}_P^H = \hat{r}_P^L = \hat{r}_P^{(0)}$, and the condition equation (A.5) corresponds to $\hat{r}_T^{(0)} \geqslant 1 + \hat{r}_P^{(0)}$.

When one takes $n \to \infty$ limit, $\hat{r}_P$ and $\hat{r}_T$ become step functions. For $\tilde{z} < 1$, the differentiation rate $\hat{r}_T = \hat{r}_T^L = 0$, the proliferative rate $\hat{r}_P = \hat{r}_P^L > 0$, and equations (9), (10) lead to $\Lambda_P^*(\tilde{z} < 1) = 1$ and $\tilde{v}_z^*(\tilde{z} < 1) = \hat{r}_P^L \tilde{z}$. On the other hand, for $\tilde{z} \geqslant 1$,

$$\Lambda_P^*(\tilde{t}) = \frac{1+\hat{r}_P^H - \hat{r}_T^H}{1+\hat{r}_P^H - \hat{r}_T^H \exp[-(1+\hat{r}_P^H - \hat{r}_T^H)\tilde{t}]}, \tag{A.6}$$

$$\tilde{v}_z^*(\tilde{t}) = \frac{\hat{r}_P^L}{1+\hat{r}_P^H - \hat{r}_T^H}\{(1+\hat{r}_P^H)\exp[(\hat{r}_P^H - \hat{r}_T^H)\tilde{t}] - \hat{r}_T^H \exp(-\tilde{t})\}, \tag{A.7}$$

where $\tilde{t}$ can be obtained by inverting the following relation

$$\tilde{z}(\tilde{t}) = 1 + \int_0^{\tilde{t}} \tilde{v}_z^*(\tilde{t}')\, \mathrm{d}\tilde{t}' = 1 + \frac{\hat{r}_P^L\{\hat{r}_T^H(\hat{r}_T^H - \hat{r}_P^H)[\exp(-\tilde{t}) - 1] - (1 + \hat{r}_P^H)(\exp[-(\hat{r}_T^H - \hat{r}_P^H)\tilde{t}] - 1)\}}{(\hat{r}_T^H - \hat{r}_P^H)(1 + \hat{r}_P^H - \hat{r}_T^H)}. \tag{A.8}$$

Several interesting quantities can be calculated from equations (A.6)–(A.8):

- Dimensionless steady state tissue height

$$\tilde{H}^* = \tilde{z}(\tilde{t} \to \infty) = 1 + \frac{\hat{r}_P^L(1 + \hat{r}_T^H)}{\hat{r}_T^H - \hat{r}_P^H} = \frac{\hat{r}_T^H(1 + \hat{r}_P^L) + (\hat{r}_P^L - \hat{r}_P^H)}{\hat{r}_T^H - \hat{r}_P^H}. \tag{A.9}$$

  Note that, since a healthy tissue should have $\tilde{H}^* \gg 1$, in the case of constant $\hat{r}_P$ ($\hat{r}_P^{(0)} = \hat{r}_P^L = \hat{r}_P^H$, the minimal model described in section 3.2), equation (A.9) requires $\hat{r}_P^{(0)}$ to be large compared to order unity. In the general case considered here, as long as $\hat{r}_P^L > \hat{r}_P^H$ (i.e., cell proliferation rate is higher in the stem-cell niche than other parts of the tissue, a condition which is very reasonable for a healthy tissue), the magnitude of $\tilde{H}^*$ is greater than that in the minimal model, and the condition for having large $\tilde{H}^*$ is the same.

- Equation (A.6) gives a characteristic time scale $\tilde{t}_c \equiv (\hat{r}_T^H - 1 - \hat{r}_P^H)^{-1}$. From this we can introduce the typical transition width h_T (normalized by the height of proliferative cell niche h_P) as

$$\frac{h_T}{h_P} \equiv \int_0^{\tilde{t}_c} \tilde{v}_z^*(\tilde{t})\, \mathrm{d}\tilde{t} = \frac{\hat{r}_P^L\{[\hat{r}_T^H(\hat{r}_T^H - \hat{r}_P^H) - (1 + \hat{r}_P^H)\exp(-1)]\exp(-\tilde{t}_c) - (1 + \hat{r}_T^H)\tilde{t}_c^{-1}\}}{(\hat{r}_T^H - \hat{r}_P^H)(1 + \hat{r}_P^H - \hat{r}_T^H)}. \tag{A.10}$$

  We can also compare h_T with the steady state tissue height H^*

$$\frac{h_T}{H^*} \equiv \frac{h_T}{h_P}\frac{1}{\tilde{H}^*} = \frac{\hat{r}_P^L\{[\hat{r}_T^H(\hat{r}_T^H - \hat{r}_P^H) - (1 + \hat{r}_P^H)\exp(-1)]\exp(-\tilde{t}_c) - (1 + \hat{r}_T^H)\tilde{t}_c^{-1}\}}{[\hat{r}_T^H - \hat{r}_P^H + \hat{r}_P^L(1 + \hat{r}_T^H)](1 + \hat{r}_P^H - \hat{r}_T^H)}. \tag{A.11}$$

  To have a sharp interface between the proliferative cell niche and the differentiated region, we need h_T/H^* to be small compared to order unity.

- Proliferative cell proportion

$$\bar{\Lambda}_P^* \equiv \frac{1}{\tilde{H}^*}\int_0^{\tilde{H}^*} \Lambda_P^* \mathrm{d}\tilde{z} = \frac{\hat{r}_P^L + \hat{r}_T^H - \hat{r}_P^H}{\hat{r}_P^L(1 + \hat{r}_T^H) + \hat{r}_T^H - \hat{r}_P^H} = \frac{1 + \frac{\hat{r}_P^L - \hat{r}_P^H}{\hat{r}_T^H}}{1 + \hat{r}_P^L + \frac{\hat{r}_P^L - \hat{r}_P^H}{\hat{r}_T^H}}. \tag{A.12}$$

To have $\bar{\Lambda}_P^*$ small compared to one when $\hat{r}_P^L \geqslant \hat{r}_P^H$, again one needs a $\hat{r}_P^L$ large compared to unity.

The results from our general model suggests that as long as $\hat{r}_P^L \geqslant \hat{r}_P^H$, for a tissue to have $H^* \gg h_P$, $h_T \ll H^*$, and $\bar{\Lambda}_P^* \ll 1$, the condition $\hat{r}_T^H \gg \hat{r}_P^L \gg 1$ should be satisfied. This is the same as the minimal model discussed in section 3.2.

ORCID iDs

Hsuan-Yi Chen https://orcid.org/0000-0002-3367-0313

References

[1] Marchetti M C, Joanny J F, Ramaswamy S, Liverpool T B, Prost J, Rao M and Simha R A 2013 *Rev. Mod. Phys.* **85** 1143
[2] Serra-Picamal X, Conte V, Vincent R, Anon E, Tambe D T, Bazelieres E, Butler J P, Fredberg J J and Trepat X 2012 *Nat. Phys.* **8** 628
[3] Banerjee S, Utuje K J C and Marchetti M C 2015 *Phys. Rev. Lett.* **114** 228101
[4] Xin T, Greco V and Myung P 2016 *Cell* **164** 1212
[5] Perez-Moreno M, Jamora C and Fuchs E 2003 *Cell* **112** 535
[6] Lander A D, Gokoffski K K, Wan F Y M, Nie Q and Calof A L 2009 *PLoS Biol.* **7** 0084
[7] Shraiman B I 2005 *Proc. Natl Acad. Sci.* **102** 3318
[8] Smart I H M 1971 *J. Anat.* **109** 243
Calof A L, Mumm J S, Rim P C and Shou J 1998 *J. Neurobiol.* **36** 190
[9] Greulich P and Simons B D 2016 *Proc. Natl Acad. Sci.* **113** 7509
[10] Lo W C, Chou C S, Gokoffski K K, Wan F Y M, Lander A D, Calof A L and Nie Q 2009 *Math. Biosci. Eng.* **6** 59
[11] Hannezo E, Prost J and Joanny J-F 2014 *J. R. Soc. Interface* **11** 20130895
[12] Snippert H J *et al* 2010 *Cell* **143** 134
[13] de Navascues J *et al* 2012 *EMBO J.* **31** 2473

[14] Turing A M 1952 *Phil. Trans. R. Soc.* B **237** 37
[15] Beites C L, Kawauchi S, Crocker C E and Calof A L 2005 *Exp. Cell Res.* **306** 309
[16] Ovadia J and Nie Q 2013 *Biophys. J.* **104** 237
[17] Schwartz L M, Chikaraishi D M and Kauer J S 1991 *J. Neurosci.* **11** 3556
[18] Mackay-Sim A and Kittel P 1991 *J. Neurosci.* **11** 919
[19] Doe C Q 2008 *Development* **135** 1575
[20] Chen S, Lewwalen M and Xie T 2013 *Development* **140** 255
[21] Delaunay D, Kawaguchi A, Dehay C and Matsuzaki F 2017 *Curr. Opin. Neurobiol.* **42** 75
[22] Proskuryakov S Y, Konoplyannikov A G and Gabai V L 2003 *Exp. Cell Res.* **283** 1
[23] van den Brink G R and Offerhaus G J 2007 *Cancer Cell* **11** 109
[24] See, for example Yeh W-T and Chen H-Y 2016 *Phys. Rev.* E **93** 052421